Available online at www.sciencedirect.com

ScienceDirect

Journal of Magnesium and Alloys 3 (2015) 79–85

www.elsevier.com/journals/journal-of-magnesium-and-alloys/2213-9567

Full length article

Optimization of mechanical and damping properties of Mg–0.6Zr alloy by different extrusion processing

Jingfeng Wang [a,b,c,*], Zhongshan Wu [a,b], Shan Gao [a,b], Ruopeng Lu [a,b], Dezhao Qin [a,b], Wenxiang Yang [a,b], Fusheng Pan [a,b]

[a] College of Materials Science and Engineering, Chongqing University, Chongqing 400044, PR China

[b] National Engineering Research Center for Magnesium Alloys, Chongqing University, Chongqing 400044, PR China

[c] The State Key Laboratory of Mechanical Transmission, Chongqing University, Chongqing 400044, PR China

Received 9 December 2014; revised 21 January 2015; accepted 2 February 2015

Available online 5 March 2015

Abstract

In this study, the optimization of mechanical and damping capacities of Mg-0.6 wt.% Zr alloys by controlling the recrystallized (DRXed) grain size under varying extrusion processing parameters including extrusion temperature T and strain rate $\dot{\varepsilon}$ was investigated. The relationship between the DRXed grain size and damping properties of the studied alloy was also discussed. The DRXed grain size of the as-extruded Mg–Zr alloys decreased as the extrusion temperature T decreased and the strain rate $\dot{\varepsilon}$ increased. As the DRXed grain size decreased, the strength and elongation of the as-extruded alloys exhibited improved performance through the grain refinement mechanism, while the damping properties deteriorated. The extrusion temperature of the Mg–Zr alloy had relatively greater effects on the mechanical and damping properties than the strain rate. The results of the present work indicate that alloys with appropriate mechanical and damping properties may be obtained from controlling the DRXed grain size by careful tailoring of the extrusion process parameters.

Keywords: Mg–Zr alloy; Mechanical properties; Damping capacities; Extrusion; Optimization

1. Introduction

As demands for lightweight, high strength, and high damping structural materials for the automobile, aerospace, and other industries have grown, damping magnesium (Mg) alloy has become one of an important direction in the research and development of Mg alloys [1–3]. Energy dissipation of pure Mg through dislocation movements occurs primarily via an internal friction mechanism. Vibrations of the dislocation loops around their equilibrium positions in Mg alloys are responsible for damping levels of about 10 times higher than those in pure aluminum [4]. With properties similar to those of traditional high-damping Mg alloys, high-damping Mg-0.6 wt.% Zr alloys were successfully developed in the 1960 s [5,8]. Recently, several studies on the damping capacities and mechanical properties of Mg–Zr alloys have been conducted by adding the alloying element yttrium and controlling the technology for heat processing and thermal deformation [6,7]. Addition of 0.5 wt.% Y generates an as-cast Mg–0.6 wt.% Zr alloy with excellent mechanical properties (σ_b = 160 MPa, $\sigma_{0.2}$ = 69 MPa, $\delta\%$ = 14.5%) and good damping capacities (loss tangent (tan φ) = 0.01 at $\varepsilon = 3.2 \times 10^{-5}$) or even better damping capacity at high strain amplitude (ε) [8]. Combination of solution treatment at 550 °C for 30 min and aging at 300 °C for 16 h effectively improves the damping capacity of

* Corresponding author. National Engineering Research Center for Magnesium Alloys, Chongqing University, Chongqing 400044, PR China. Tel.: +86 23 65112153.

E-mail address: jfwang@cqu.edu.cn (J. Wang).

Peer review under responsibility of National Engineering Research Center for Magnesium Alloys of China, Chongqing University.

http://dx.doi.org/10.1016/j.jma.2015.02.001.

Mg–Zr alloys for the crucial role of twin structures in the alloy matrix [9]. Dong et al. [10,11] systematically studied the microstructures and properties of Mg–Zn–Y–Zr alloys by using heat treatment, extrusion and modification. However, there are seldom studies to discuss the optimization of the mechanical and damping properties of Mg–Zr alloys by using different extrusion parameters. Moreover, although alloy strengthening, heat treatment strengthening, deformation strengthening, composite strengthening and other enhancement methods have been applied to improve the alloy performance, these procedures are unable satisfy the increasing rigorous demands of rapidly advancing modern industries.

Because of the relationship between mechanical properties and damping capacities is contradictory, the comprehensive properties of an alloy are difficult to control [12]. The effects of microstructures on the alloy properties have been experimentally investigated, but theoretical relations to the appropriate references have not been described. To predict results as accurately as possible, directionally designing technological processing parameters is important. Here, investigations of the relationships among macro-process parameters, microstructures, and alloy properties are of theoretical and practical significance.

In the present work, the optimization of the microstructures, mechanical and damping capacities of Mg-0.6 wt.% Zr alloy was investigated by discussing the relationships among extrusion parameters, the average recrystallized grain size and properties. It is hoped that knowledge of the relationships among the macro-process parameters, micro-structure, and capacities will provide theoretical information relevant to the hot extrusion processing of high damping lightweight Mg–Zr alloys.

2. Experimental procedures

Mg-0.6 wt.% Zr alloy ingots with a diameter of 252 mm were prepared from commercial pure Mg (99.99 wt.%) and Mg–30%Zr master alloy through semi-continuous casting and protected by 0.2% SF_6+99.8%CO_2 mixed gas. First, the ingots were homogenized at 350 °C for 3 h and then extruded in a 2,500 t of YA32-315 four-column versatile hydraulic press. Extrusion was conducted by varying two kind of different extrusion parameters, namely, extrusion temperature and extrusion speed, which were 330 °C, 9.6 mm/s, 330 °C, 5.3 mm/s and 400 °C, 5.3 mm/s for alloy I, alloy II and alloy III, respectively. The equivalent strain rate during extrusion was estimated according to [13]:

$$\dot{\varepsilon} = \frac{6VD_0^2 \ln R_e \tan\phi}{D_0^3 - D_e^3} \quad (1)$$

where V is the ram speed, D_0 is the container diameter, D_e is the extrusion die diameter, Re is the extrusion ratio ($Re = D_0^2/D_e^2$), and ϕ is the semi-angle of the conical die. The extrusion speed can be converted into strain rate $\dot{\varepsilon}$, which is one of the Zener–Hollomon parameters. The values of extrusion temperature T and strain rate $\dot{\varepsilon}$ are shown in Table 1.

Table 1
The extrusion temperature T and strain rate $\dot{\varepsilon}$ of Mg–Zr alloys.

Alloy codes	Alloy I	Alloy II	Alloy III
T	330 °C	330 °C	400 °C
$\dot{\varepsilon}$	0.45/s	0.25/s	0.25/s

The microstructures and phase constitutions of the specimens were examined by Olympus optical microscope and X-ray diffraction (XRD). Tensile testing at ambient temperature was performed using a Shimadzu CMT-5105 material testing machine with a stretching rate of 3 mm/min. The damping samples were machined to dimensions of 45 mm × 5 mm × 1 mm parallel to the extrusion direction using an electric spark cutter. The damping capacity was determined through dynamic mechanical analysis (TA-DMA Q800) in single cantilever vibration mode with a measurement frequency of 1 Hz and various strain amplitudes ε ranging from 6×10^{-5} to 6×10^{-3} and the loss tangent (tan φ). Given that tan φ is equivalent to the inverse quality factor (Q^{-1}) when the internal friction is very low, the damping capacities of the alloys were evaluated using Q^{-1} as a substitute for tan φ.

3. Results and discussion

3.1. Microstructures of the Mg–Zr alloys

The transverse sectional microstructures of the alloys I, II, III are shown in Fig. 1(a)–(c). Usually, the extrusion process rarely changes the phase composition of the alloy, so only alloy III was selected to do the X-ray diffraction experiment, which is shown in Fig. 1d. From the XRD pattern, the main phases of as-extrusion Mg–Zr alloy are α-Mg solid solution and α-Zr phase. There is no formation of alloy phase due to the small solid solubility of Zr element in Mg matrix. Hence, the phase constitution has little impact on the properties of the Mg–Zr alloy. From the metallographical of the three alloys, it can be seen that after extrusion, the original grains of the Mg–Zr alloy are seriously crushed, due to the effects of extrusion stress, and meanwhile, a large number of dynamic recrystallized (DRXed) grains appear and mix with the seriously deformed grains. On the one hand, the recrystallized grain sizes is different because of their different extrusion parameters, namely, extrusion temperature and strain rate. Alloys I and II were extruded at 330 °C, alloy III was extruded at 400 °C. As is well known that, the higher extrusion temperature is, the more easily recrystallization will occur, and grains tend to grow up, so the grain size of alloy III is larger than that of alloys I and II. On the other hand, under lower extrusion temperature of 330 °C, alloy I has a higher extrusion rate of 9.6 mm/s than alloy II. The lower extrusion rate is, the more work will be done by the extrusion stress. Therefore, the recrystallized grains of alloy II under lower extrusion rate have more energy and are able to grow larger. Consequently, the grain size of the alloy I was smaller than those of alloys II and III. Based on the metallographs shown in Fig. 1, the calculated average grain sizes of alloy I, alloy II and alloy III were approximately 21, 30, and 70 μm, respectively.

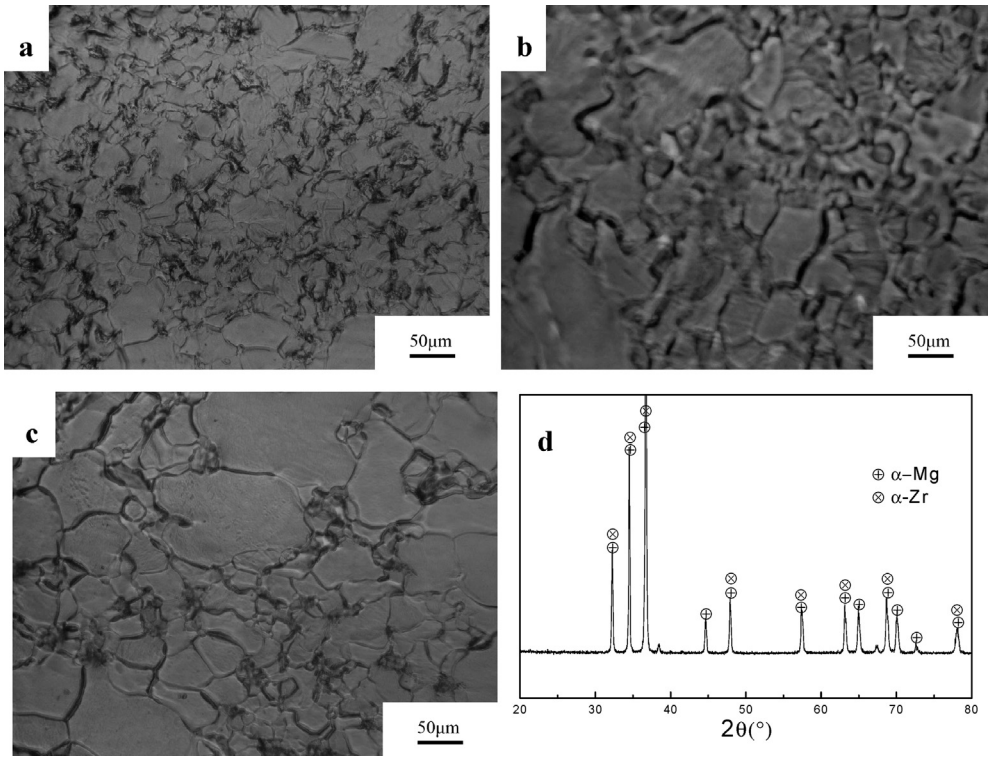

Fig. 1. The microstructures of Mg–Zr alloys: (a) Alloy I, (b) alloy II, (c) alloy III and (d) XRD pattern of the alloy III.

3.2. Properties of the Mg–Zr alloys

Fig. 2 and Table 2 show the tensile strength σ_b, yield strength $\sigma_{0.2}$ and elongation δ of the as-extruded Mg–Zr alloys (alloys I-III). It can be found that alloy I with the smallest grains had the highest yield strength. By contrast, alloy III with the largest grains had the lowest yield strength. For alloy II, its presented moderate grain sizes and yield strength. And the ultimate strengths of the alloys coincided with their yield strength. According to grain refinement strengthening theory, grain size directly affects on the mechanical properties of an alloy. Under applied stress, plastic deformation could be easily transmitted to adjacent grains and alloys with finer grains would exhibit higher yield strength because of lower local stress concentration in the smaller grains. In terms of the Hall–Petch equation: $\sigma = \sigma_0 + kd^{-1/2}$, the yield strength is inversely proportional to the square root of the grain size [14]. In addition, with the decrease of grain size, the plasticity of materials is also significantly improved, which is well consistent with the strength variation of the alloys shown in Fig. 2. Under the same external stress, a smaller strain difference between the grain boundary and intra-grain in finer grain alloys reduces the possibility of crack initiation and extension resulting from local stress concentration. Thus, alloy I, which has the smallest average grain size among the studied alloys, exhibited the highest elongation. In a word, grain sizes consistently decreased whereas strengths and plasticity generally increased from alloy III, alloy II to alloy I.

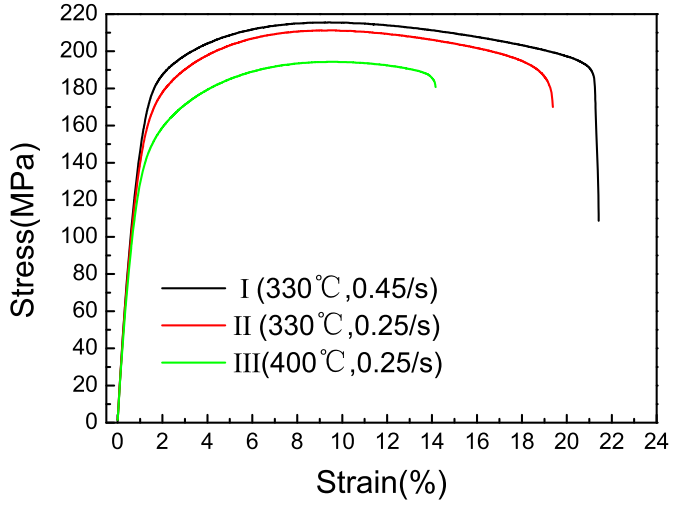

Fig. 2. Mechanical properties of as-extruded Mg–Zr alloys under different extrusion parameters.

The damping capacities of Mg–Zr alloys obtained under different extrusion parameters at room temperature as a function of varying strain amplitudes from 5×10^{-4} to 3×10^{-3} is shown in Fig. 3. The x- and y-axes correspond to the strain amplitude (ε) and loss tangent ($\tan \varphi = Q^{-1}$), respectively. The curves observed may be divided into two regions by critical strain amplitude (ε_{cr}) of 2.0×10^{-4}. In the first region, in which strain amplitude is below the critical value, the Q^{-1} values of all alloys at low strain amplitude are small and hardly distinct with varying the strain amplitude. Nonetheless, the damping value of alloy III achieves a high damping standard (Q^{-1} >0.01). However, above the critical strain amplitude ε_{cr} of each curve, the damping values of the

Table 2
Extrusion parameters, tensile properties, and damping capacities of the extruded alloys.

No.	Extrusion parameters			DRX size	Tensile properties			Damping
	T(°C)	$\dot{\varepsilon}$ (s^{-1})	Z parameter	d (μm)	σ_b(MPa)	$\sigma_{0.2}$ (MPa)	EL(%)	Q^{-1} ($\varepsilon = 5 \times 10^{-4}$)
I	330	0.45	2.2422×10^{11}	21	216	165.7	20.8	0.01782
II	330	0.25	1.2457×10^{11}	30	211	154.9	18.4	0.01843
III	400	0.25	7.5681×10^{9}	70	192	136.4	15.6	0.02012

three alloys remarkably increased with increasing the strain amplitude.

For Mg alloys, energy dissipation by dislocation movements is the major internal friction mechanism. According to the G-L dislocation pinning model [15], at low temperatures, damping of Mg alloys at ambient temperature is produced by moving dislocations and point defects. With a slight excess of alternating stress, mobile dislocations are pinned by weak pinning points and the bow between neighboring points with short distances, thereby generating low internal friction in the alloys; this stage is called strain-independent damping. However, once the strain amplitude exceeds a critical value, mobile dislocations break away from weak pinning points, inducing the "avalanche form" phenomenon and rapidly increasing the internal friction. When the stress is unloaded, the dislocation loops elastically shrink and are finally pinned by point defects. During the unpinning process and rebounding of dislocation loops, static hysteresis internal friction is generated; this stage is referred to as strain-dependent damping. Therefore, the damping capacity of alloys can be divided into two parts: the first includes strain-independent damping represented by Q_0^{-1} and the second includes strain-dependent damping expressed as $Q_h^{-1}(\varepsilon)$ [15]:

$$Q^{-1}(\varepsilon) = Q_o^{-1} + Q_h^{-1}(\varepsilon) \quad (2)$$

In Fig. 3, there is scarcely obvious distinction for the Q_0^{-1} values of the alloys obtained under different extrusion parameters in the low strain amplitude region. However, once the strain amplitude surpasses the critical value, the Q_h^{-1} values of all of the alloys begin to accelerate with the increase of strain amplitude. In the low strain amplitude region, the damping capacity of alloy III is the most remarkable among the three alloys. The damping value of alloy II is slightly higher than that of alloy I. It can be found that the performances of the three alloys are in agreement with the general finding that damping capacities and mechanical properties are contradictory [12].

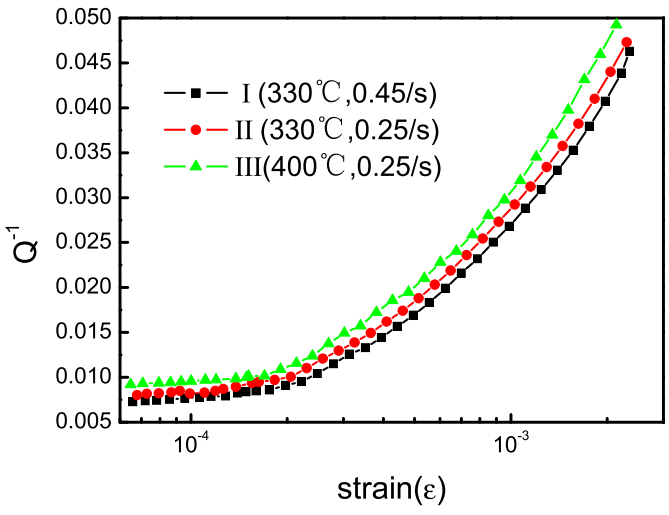

Fig. 3. Damping capacities of as-extruded Mg–Zr alloys.

3.3. Optimization of mechanical and damping properties of the Mg–Zr alloys

During Mg alloy processing, changes in mechanical properties mainly depend on the variations in grain size, namely, the grain refinement strengthening. However, fine grains could lead to large areas of grain boundaries, and oscillation of dislocations is strongly hindered. Furthermore, the grain boundary sliding of fine grains would become more difficult. Then, all of these considerations have significant effects on the damping capacities of the alloys. Therefore, the present study focused on controlling the grain size and optimizing the mechanical properties and damping capacities of the alloys by manipulating the extrusion parameters.

During extrusion, variations in the extrusion parameters directly influenced the grain size of the alloys. From the analyses described above, recrystallized grain sizes considerably affect the mechanical properties of the resultant alloys. To investigate the relationship between microstructures and mechanical properties of the alloys, there have been many studies on the relationships between the recrystallized grain size and the extrusion parameters of temperature and strain rate [17,18]. It is well known that the Zener–Hollomon parameter (Z parameter) is a useful variable for explaining this relationship [19], which consists of a combined function of temperature and strain rate, this parameter can be expressed as

$$Zd^m = A \quad (3)$$

$$Z = \dot{\varepsilon}\exp\left(\frac{Q}{RT}\right) \quad (4)$$

where d is the average DRXed grain size, m is the grain size exponent, A is a constant, $\dot{\varepsilon}$ is the strain rate, Q is the lattice diffusion activation energy of Mg (135 kJ/mol), R is the universal gas constant (8.31 J/(mol K)), and T is the extrusion temperature. The equation shows that both the increase of strain rate and the decrease of deformation temperature could refine the grain size. In the present study, the deformation temperature of alloy I was lowest and its strain rate was

fastest, so its grain size was smallest among the alloys studied. The properties of the two other alloys are also consistent with this rule. The Z parameter and the strain rate under the extrusion conditions employed in this study were obtained from Eqs. (1) and (4), respectively, and the tensile properties and damping capacities of the extruded alloys are listed in Table 2.

Similar to the previous study [20], the DRXed grain size (d) could be expressed as a function of the Z parameter through the relation $\ln d = B - m \ln Z$ with B and m values of 11.97 and 0.34, respectively, for the Mg–Zr alloys according to Eq. (3) and as shown in Fig. 4. In order to discuss the influence of extrusion parameters on the DRXed grain size, the relationship between the DRXed grain size and Zener–Hollomon parameter is shown in Fig. 4. According to Eq. (4) and Fig. 4, the increase of the strain rate results in a decrease in the size of the DRXed grains, while an increase of the extrusion temperature leads to an increase in the DRXed grain size. It is commonly known that the DRXed grain size increases as the temperature increases and the strain rate decreases. Moreover, it is amazing to note that the extrusion temperature has great effect on the DRXed grain size while the strain rate has a relatively small effect according to Table 2. This phenomenon has also been observed in the ZK60 alloys [19].

In addition, the relationship between the DRXed grain size and tensile properties is presented in Fig. 5a. A linear proportional relationship in which an increase in the DRXed grain size causes poorer mechanical capacities may be observed. The grain refinement mechanism is usually attributed to this phenomenon [20]. And the smaller extrusion temperature exhibits excellent mechanical properties under the same extrusion conditions combine with Table 2 and Fig. 5a, and coincides with the previous discussion. Fig. 5b shows the relationship between the yield strength and the average DRXed grain size of the as-extruded Mg–Zr alloys. The relationship observed corresponded well with the Hall–Petch relation and may be expressed as follows

$$\sigma = 100.9 + 296.5 d^{-1/2} \tag{5}$$

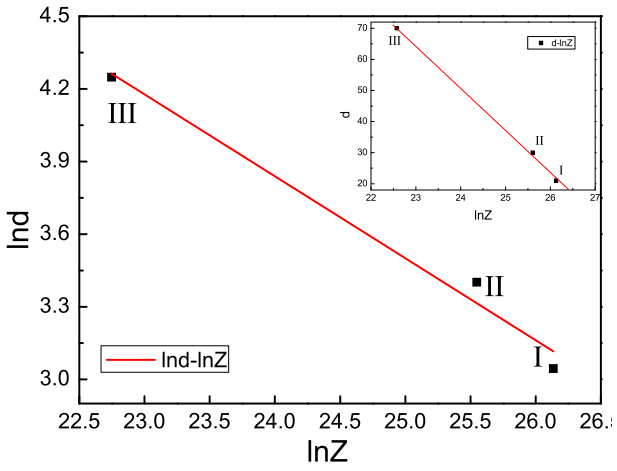

Fig. 4. Relationship between DRXed grain sizes and the Zener–Hollomon parameter.

where σ is the yield strength and d is the DRXed grain size. Interestingly, the extrusion parameters directly and significantly influenced the DRXed grain size, and the DRXed grain size considerably affected the mechanical properties. Therefore, the mechanical properties of the studied alloys may be controlled by adjusting the macro-extrusion parameters (T and$\dot{\varepsilon}$) before processing.

Fig. 6 shows the G-L plots (i.e., $\ln(\varepsilon \cdot Q_h^{-1})$ vs. $1/\varepsilon$) of the as-extruded Mg–Zr alloys generated from the experimental data. It can be found that the slopes of the three alloys are observed to be mainly consistent. Based on the G-L dislocation pinning model, at the high strain amplitude region, the static hysteresis internal friction, namely, strain-dependent damping, is generated from the unpinning process and rebounding of dislocation loops, which could be expressed as Eq. (6) [16]:

$$Q_h^{-1} = \frac{C_1}{\varepsilon} \exp\left(-\frac{C_2}{\varepsilon}\right) \tag{6}$$

In this equation, $C_1 = \Omega \Lambda L_N^3 K \eta \alpha / \pi^2 L_C^2$, $C_2 = K \eta \alpha / L_C$, ε is the amplitude of strain, Ω is the orientation factor, K is a factor related to the anisotropy of the elasticity coefficient and sample orientation, η is the mismatch coefficient of the solute and solvent atoms, α is the lattice constant, L_N is the length between the strong pinning points in a dislocation, and L_C is the length between the weak pinning points in a dislocation. This equation also could be rewritten as:

$$\ln\left(\varepsilon \cdot Q_h^{-1}\right) = \ln C_1 - C_2 \varepsilon^{-1} \tag{7}$$

Eq. (7) demonstrates that $\ln(\varepsilon \cdot Q_h^{-1})$ and $1/\varepsilon$ have a linear relationship; here, the slope corresponds to the C_2. A large intercept and smaller slope lead to better damping capacity. From Eq. (7), the relationship between $\ln(\varepsilon \cdot Q_h^{-1})$ and $1/\varepsilon$ should be linear, that the intercept is $\ln C_1$, and that the slope is $-C_2$. Then, this linear relationship suggests that the damping behavior of the three alloys is in agreement with G-L theory. Given that the Lc values are hardly distinguishable among the alloys, the corresponding C_2 values also do not change according to Eq. (7). Therefore, the G-L plots of the test alloys have the same slopes. On the other hand, as the main impact factor of the value of C_1, L_N significantly influences the Q_h^{-1} values according to Eq. (6) and is directly affected by the grain boundaries [21]. As the pinning effects of the strong pinning points in a dislocation are dominated by the grain boundaries because no other second phase particles are present in the test alloys, L_N values would mainly depend on the distance of grain boundaries, namely, the average grain size. Hence, according to Eq. (6) and Eq. (7), $\ln C_1$, which is the intercept of the G-L plots, is directly proportional to the average grain size of the alloys. As a result, the G-L plot of alloy III which has the largest average grain size, showed the largest intercept. The G-L plot intercepts of alloys II and I also exhibited similar variation tendencies with decreasing average grain size. Considering the identical slopes of the G-L plots, a high intercept would indicate the excellent damping capacity of an alloy. Thus, as indicated in Fig. 6, alloy III, which features the highest intercept, showed the best damping capacity.

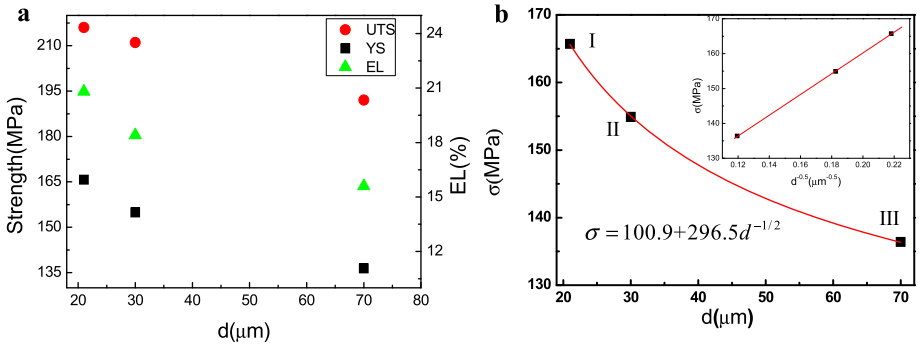

Fig. 5. (a) Relationship between recrystallized grain size and tensile properties and (b) the variation of tensile yield strength with the recrystallized grain size (i.e.,Hall–Petch relation).

The damping capacity of alloy II, which has a moderate intercept, was slightly better than that of alloy I, which presents the lowest intercept among the alloys studied.

Combined with the previous discussion, the higher extrusion temperature of the Mg–Zr alloy exhibits the excellent damping capacity while the strain rate has not obvious effected on the damping property under the same extrusion conditions from Fig. 3. This may be mainly due to the higher extrusion temperature of the Mg–Zr alloy has larger DRXed grain size. Consequently, the extrusion temperature of the Mg–Zr alloy has relatively greater effects on the mechanical and damping properties than the strain rate from all above. Fig. 7 shows fitting curves of the relationship between the damping property Q^{-1} and average DRXed grain size d at different strain amplitude. It suggests that the linear proportional relation between them. And it is amazing to note that the damping values at all strain amplitude increased slowly as the average DRXed grain size increased. This effect is attributable to the L_N values, which mainly depend on the average distance of grain boundaries, namely, the average grain size d. Considering that the average DRXed grain size is directly affected by the extrusion process, control of the damping properties of alloys is possible by tailoring the extrusion parameters T and $\dot{\varepsilon}$ before extrusion.

The relationship between the DRXed grain size and properties of Mg–Zr alloys is presented in Fig. 8. The contradictory relationship between the damping capacity and strength of the Mg–Zr alloys may be clearly observed. It also suggests that the strength of the studied alloys significantly decreased as the DRXed grain size increased, while the damping capacity relative slightly increased as the DRXed grain size increased. It is necessary to control the finer grain by adjusting the lower extrusion temperature and higher strain rate in need of higher strength and lower damping capacity, and vice versa. Then, the excellent moderate capacities of the Mg–Zr alloys may be obtained when the DRXed grain size of the Mg–Zr alloy nearby a value according to the fitting curves. Thus, it is requirement to control the DRXed grain size by setting the extrusion parameters in order to obtain the balance optimization of mechanical and damping capacities of the Mg–Zr alloys. Therefore, tailoring of the extrusion parameters may be an important approach for adjusting the mechanical and damping performances of Mg–Zr alloys. It is potentially hoped that the results will contribute to the preparation of high strength and high damping structural materials designs of magnesium alloy for anti-vibration and noise-reduction applications.

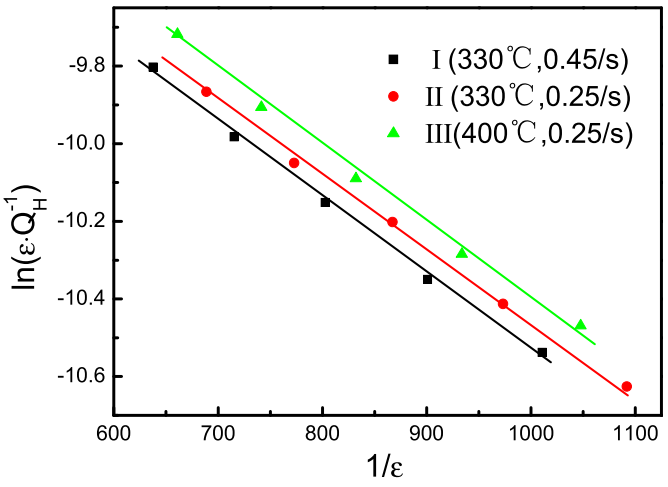

Fig. 6. G-L plots of the Mg–Zr alloys.

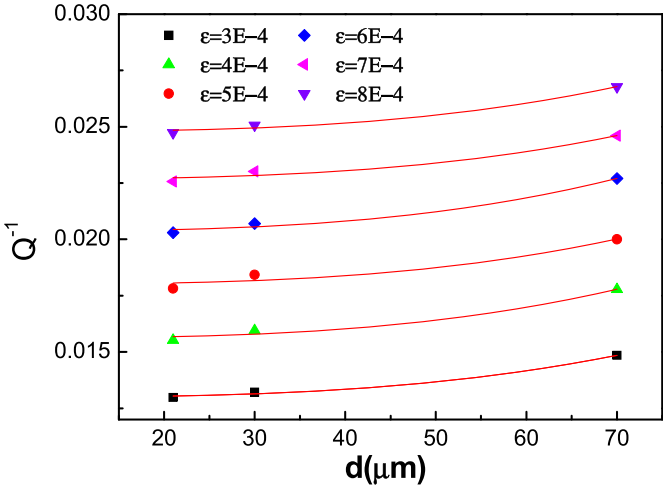

Fig. 7. Relationship between DRXed grain size and damping properties of the Mg–Zr alloys.

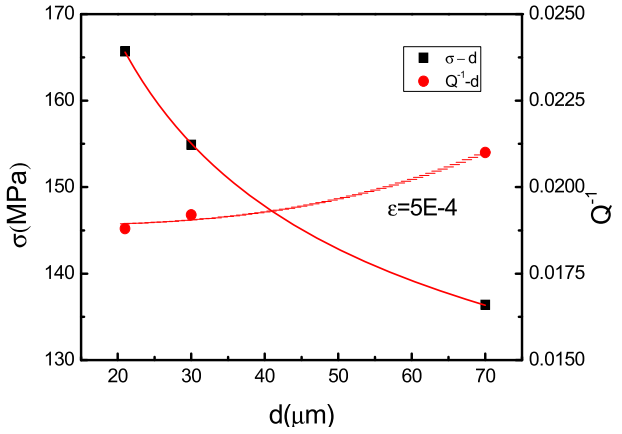

Fig. 8. Relationship between DRXed grain size and properties of the Mg–Zr alloys.

4. Conclusions

In summary, optimization of mechanical and damping capacities of Mg-0.6 wt.% Zr alloys by controlling the recrystallized (DRXed) grain size under varying extrusion processing parameters including extrusion temperature T and strain rate $\dot{\varepsilon}$ were researched synthetically. Three main conclusions can be drawn as follows:

1) The Mg–Zr alloy extruded at a temperature of 330 °C and the strain rate of 0.45/s exhibited a DRXed homogenous microstructure. The DRXed grain size of the as-extruded Mg–Zr alloys decreased as the temperature decreased and the strain rate increased.
2) With the decrease of the DRXed grain size, the strength and elongation of the as-extruded alloys increased, while the damping capacity relative slightly decreased. The extrusion temperature of the Mg–Zr alloy had relatively greater effects on the mechanical and damping properties than the extrusion strain rate.
3) The DRXed grain size was directly influenced by the extrusion parameters, and it significant affected the mechanical and damping properties of the Mg–Zr alloy. Thus, it is requirement to control the DRXed grain size by setting the extrusion parameters in order to obtain the appropriate capacities of the Mg–Zr alloys.

Acknowledgments

The authors are grateful for the financial support from the foundation support of the Key Laboratory of Science and Technology on High Energy Laser, CAEP, the National Natural Science Foundation Commission of China (Grant No. 51271206), the National Basic Research Program of China (Grant No. 2013CB632201), and the Program for New Century Excellent Talents in University (Grant No. NCET-11-0554).

References

[1] L.H. Wen, Z.S. Ji, M.L. Hu, H.Y. Ning, J. Magnesium Alloys 2 (2014) 85–91.
[2] J.H. Jun, J. Alloys Compd. 610 (2014) 169–172.
[3] Tao Li, Yong He, Hailong Zhang, Xitao Wang, J. Magnesium Alloys 2 (2014) 181–189.
[4] A.S.M.F. Chowdhury, D. Mari, R. Schaller, Acta Mater. 58 (2010) 2555–2563.
[5] Z.L. Liu, X.Q. Liu, P. Shen, X.R. Zhu, L. Meng, Trans. Nonferrous Met. Soc. China 20 (2010) 2092–2095.
[6] J.F. Wang, P.F. Song, S. Gao, X.F. Huang, Z.Z. Shi, F.S. Pan, Mater. Sci. Eng. A 528 (2011) 5914–5920.
[7] D. Wu, Y.Q. Ma, R.S. Chen, W. Ke, J. Magnesium Alloys 2 (2014) 20–26.
[8] D.Q. Wan, J.C. Wang, G.C. Yang, Mater. Sci. Eng. A 517 (2009) 114–117.
[9] M.H. Tsai, M.S. Chen, L.H. Lin, M.H. Lin, C.Z. Wu, K.L. Ou, C.H. Yu, J. Alloys Compd. 509 (2011) 813–819.
[10] B.S. Yan, X.P. Dong, R. Ma, S.Q. Chen, Z. Pan, H.J. Ling, Mater. Sci. Eng. A 594 (2014) 168–177.
[11] R. Ma, X.P. Dong, B.S. Yan, S.Q. Chen, Z.B. Li, Z. Pan, H.J. Ling, Z.T. Fan, Mater. Sci. Eng. A 602 (2014) 11–18.
[12] J.F. Wang, R.P. Lu, W.W. Wei, X.F. Huang, F.S. Pan, J. Alloys Compd. 537 (2012) 1–5.
[13] L.B. Tong, M.Y. Zheng, L.R. Cheng, S. Kamado, H.J. Zhang, Mater. Sci. Eng. A 569 (2013) 48–53.
[14] Vladimir Bata, Elena V. Pereloma, Acta Mater. 52 (2004) 657–665.
[15] G.Y. Lin, Z.F. Zhang, H. Zhang, D.S. Peng, J. Zhou, Acta Metall. Sin. 21 (2008) 109–115.
[16] S.W. Xu, S. Kamado, N. Matsumoto, T. Honma, Y. Kojima, Mater. Sci. Eng. A 527 (2009) 52–60.
[17] H. Yu, S.H. Park, B.S. You, Y.M. Kim, H.S. Yu, S.S. Park, Mater. Sci. Eng. A 583 (2013) 25–35.
[18] S.S. Park, B.S. You, D.J. Yoon, J. Mater. Pro. Technol. 209 (2009) 5940–5943.
[19] A. Granato, K. Lucke, J. Appl. Phys. 27 (1956) 583–593.
[20] A. Granato, K. Lucke, J. Appl. Phys. 27 (1956) 789–809.
[21] H. Zhou, J.F. Wang, F.S. Pan, D.D. Xu, A.T. Tang, H. Liang, Trans. Nonferrous Met. Soc. China 23 (2013) 1610–1616.